Vol. 176: 215–230, 1999 | MARINE ECOLOGY PROGRESS SERIES
Mar Ecol Prog Ser | Published January 18

Carbon cycling in a large coastal embayment, affected by wind-driven upwelling: short-time-scale variability and spatial differences

Gabriel Rosón[1,*], X. A. Álvarez-Salgado[2], Fiz F. Pérez[2]

[1]Facultad de Ciencias del Mar, Universidad de Vigo, Apartado 874, E-36200 Vigo, Spain
[2]Instituto de Investigacións Mariñas, C.S.I.C., Apartado 2026, E-36208 Vigo, Spain

ABSTRACT: Carbon species fluxes and net budgets were studied with a 2-D box model in the Ría de Arousa (Spain), a large indentation in the NW Iberian upwelling system. The embayment acted as a CO_2 source to the atmosphere during the upwelling season (average CO_2 flux across the seawater-air interface, F_{CO_2} = +16 mg C m^{-2} d^{-1}), despite the elevated net community production (NCP) rates (average NCP = 0.84 g C m^{-2} d^{-1}). The high pCO_2 levels in source Eastern North Atlantic Central Water (ENACW) and the reduced residence times within the Ría (~6 d) seem to be the reasons for the observed F_{CO_2}. The CO_2 increase associated with $CaCO_3$ fixation by the intensive culture of mussels on hanging ropes did not affect F_{CO_2} significantly. High F_{CO_2} values were observed during strong upwelling, which was 3 times larger than the average during the upwelling season. Under these conditions the CO_2-rich source ENACW reached the surface and this coincided with low phytoplankton production (NCP = −0.01 g C m^{-2} d^{-1}). Source ENACW was enriched within the Ría with carbon released from the sediments. F_{CO_2} was reduced to ⅓ of its value compared to the average upwelling season under conditions of moderate upwelling. Phytoplankton grew rapidly (average NCP = 1.49 g C m^{-2} d^{-1}) at the expense of the gentle injection of new nutrients at the base of the pycnocline. Negligible F_{CO_2} values were observed during upwelling relaxations, when ENACW into the Ría was replaced by the warm and CO_2-equilibrated shelf surface waters. F_{CO_2} reached a maximum during a strong autumn downwelling event because of the concurrence of warm shelf surface water flow into the Ría with strong carbon release from the sediments. CO_2 fluxes per unit area always increased coastwards, because of the progressive CO_2 enrichment of the source ENACW as it enters the embayment and the decrease of residence times.

KEY WORDS: Carbon fluxes · Biogeochemical cycling · Upwelling stress-relaxation · Downwelling · Rías Baixas (NW Spain)

INTRODUCTION

The study of ocean carbon fluxes is one of the keystones for obtaining knowledge of climatic changes, since ~30% of anthropogenic emissions of CO_2 seems to have been trapped by the oceans (Watson et al. 1993). CO_2 fluxes across the seawater-air interface in open ocean regions are highly variable: the ocean functions as an efficient CO_2 sink at high latitudes, whereas it is a net CO_2 source at the low-latitude equatorial upwelling regions (Takahashi et al. 1986). Special attention has been paid to ocean margins during the last decade. They support an important fraction of the global primary production (18 to 33%), although they cover only ~8% of the total ocean surface (Wollast 1991, 1993). In addition, as much as 83% of carbon mineralization and 87% of carbon burial in marine sediments occur in coastal regions (Middleburg et al. 1993). Coastal upwelling areas are of major interest because the enhanced nutrient input to the photic layer intensifies CO_2 uptake by primary producers as well as export fluxes of the produced, dissolved, and particulate organic carbon (Walsh 1991, Wollast 1993).

The NW Africa upwelling system embraces the western coast of the Iberian Peninsula (Wooster et al.

*E-mail: groson@uvigo.es

Table 1. Glossary of relevant terms

C_i	Concentration of any carbon species in a convective flow (Q_X, Q_{X0}, Q_Z)
C_R	Concentration of any carbon species in the river flow (R)
C_U, C_L	Concentration of any carbon species in the lower and upper layer of a box
D	Flux of any carbon species carried by the turbulent diffusion flow (M_Z)
ENACW	Eastern North Atlantic Central Water
F_{CO_2}	CO_2 flux across the seawater-air interface
F_E	Flux of any carbon species associated to the 'boundary movement' (Q_E)
F_{Q_i}	Flux of any carbon species carried by a convective flow (Q_X, Q_{X0})
F_R	Flux of any carbon species carried by the river flow (R)
F_Z	Flux of any carbon species carried by vertical convective flow (Q_Z)
H	Heat exchange flux across the seawater-air interface
$i - o$	Net daily budget of inputs minus outputs in a box for any carbon species
$I - O$	Average $i - o$ between 2 consecutive surveys
I_W	Upwelling index
k	Piston velocity
M_Z	Turbulent diffusion flow
NCP	Net community production
pCO_2, $pCO_{2_{ATM}}$	Partial pressure of CO_2 at the sea surface and in the atmosphere
Q_X, Q_{X0}	Upper and lower horizontal convective flows
Q_Z	Vertical convective flow
Q_E	Net upward movement of the boundary between upper and lower layer
R, P, E	River flow, precipitation and evaporation rates
S_{CO_2}	Solubility of CO_2
V	Volume of any box in the Ría de Arousa
W_C	Net particulate organic carbon deposition to the sediment
W_P	Net particulate total phosphorus deposition to the sediment
$\Delta CaCO_3$	Net calcium carbonate fixation
ΔDIP	Net dissolved inorganic phosphorus production
ΔDOC	Net dissolved organic carbon production
ΔNO_3^-, ΔNO_2^-, ΔNH_4^+	Net nitrate, nitrite and ammonium production
ΔPOC	Net particulate organic carbon production
ΔPTP	Net particulate total phosphorus production
$\Delta TIC'$	Net inorganic carbon production
$\Delta TA'$	Net total alkalinity production

1976), where upwelling-favourable winds prevail during spring and summer (the upwelling season; Blanton et al. 1987). The 'Rías Baixas', which is composed of 4 large coastal embayments in NW Spain, function as an extension of the shelf during the upwelling season (Rosón et al. 1995, Doval et al. 1997). Thus, water circulation can be modelled with a 2-D approach (Prego & Fraga 1992, Rosón et al. 1997), compared with the more complex 3-D problem in open shelves affected by upwelling (Smith 1983).

To study carbon and nutrient cycling in ocean margins affected by wind-driven upwelling, an intensive research programme was developed in the Ría de Arousa from May to October 1989. The main goals were to monitor the spatial and temporal variability associated with upwelling episodes, to quantify the effect of upwelling on the water circulation pattern, and to determine the fluxes and net budgets of biogenic constituents. Within this framework, the present paper is devoted to the spatial differences in fluxes and net budgets of carbon species (obtained with a 2-D box model using published data) at the seasonal and short (3 to 4 d) time scales. After the companion papers by Álvarez-Salgado et al. (1996a, b) on the nitrogen cycle, we focus on specific issues of the carbon cycle: (1) the partitioning of the carbon trapped into the embayment between organic (net community production, NCP) and inorganic ($CaCO_3$) forms; and (2) the CO_2 exchange across the seawater-air interface, to evaluate the efficiency of the Ría de Arousa as a sink for anthropogenic CO_2.

MATERIALS AND METHODS

Previous work. Basic information on the biogeochemistry of the rías at the short-time-scale has been gained from the intensive sampling in the Ría de Arousa. It has been demonstrated that heat exchange across the seawater-air interface and freshwater discharge contributed to stratification in the surface layer. Conversely, periodic (14 ± 4 d) wind-driven, upwelling pulses forced cold, salty, nutrient- and CO_2-rich ENACW to move into the deep layer of the Ría. Upwelling eroded the pycnocline with a resultant exchange of ENACW to the surface (Rosón et al. 1995). Accordingly, water flows, calculated with a 2-D box model (Rosón et al. 1997), were coupled with I_W ($r^2 \approx 0.50$). Reversal of the circulation occurred during downwelling periods, with the advection of warm, nutrient- and CO_2-poor shelf surface water. This shelf water occupied the entire water column, displacing the water flowing into the Ría along the bottom to the shelf. Additional nutrient and CO_2 enrichment of ENACW that entered the rías occurred on the shelf, due to the mineralization of sinking particulate organic matter (Álvarez-Salgado et al. 1993). The periodic stress/relaxation sequence determined microplankton species composition inside the Ría, which resulted in annual succession from small pioneer diatoms to red-tide species, which occur several times during the

upwelling season (Pazos et al. 1995). The contribution of freshwater to the water flow (Rosón et al. 1991) and element fluxes (Pérez et al. 1992) in the Ría were minor during this period.

Knowledge of water flow and nitrogen concentrations allowed Álvarez-Salgado et al. (1996a, b) to determine the spatial and short-time-scale change in fluxes and budgets of nitrogen species. They observed that NCP rates were linked to I_W, with maximum values due to the supply of external nitrate after strong upwelling events, and minimum values after periods of prolonged relaxation, when ammonium accumulated in the Ría. The culture of mussels on hanging ropes had a major impact on nitrogen biogeochemistry enhancing the formation of dissolved organic nitrogen. In addition, these authors summarised the observed hydrographic variability in 4 representative periods: (I) upwelling after high stratification (June 26 to July 17); (II) upwelling after low stratification (August 31 to September 11); (III) upwelling relaxation (August 7 to 17); and (IV) autumn downwelling (October 13 to 30). These contrasting short periods will be revisited here to study the spatial variability of carbon cycle species in the different segments of the Ría.

The 2-D box model. A glossary of the relevant terms used here is given in Table 1.

Input data for the model: The Ría de Arousa was surveyed twice a week from 12 May to 30 October 1989. Water samples were collected at 10 fixed stations (Fig. 1) from 5 to 7 depths, using 5 l Niskin bottles equipped with reversing thermometers. Salinity, nitrate, nitrite, ammonium, phosphate, pH-NBS, total alkalinity (TA), and particulate organic carbon and phosphorus were determined by standard methods (Rosón et al. 1995, Álvarez-Salgado et al. 1996a). Total inorganic carbon (TIC) and CO_2 partial pressure (pCO_2) were calculated from TA and pH using the carbonic acid constants of Mehrbach et al. (1973) and the solubility constant of Weiss (1974). In addition, we collected daily data on (1) river flows, taken from the gauge stations in rivers Ulla and Umia (Rosón et al. 1991); (2) precipitation rates, from the Meteorological Observatory in Villagarcía de Arousa (Fig. 1); and (3) the wind speed 10 m above the sea surface, which was measured with an anemometer placed at the main mast of the vessel.

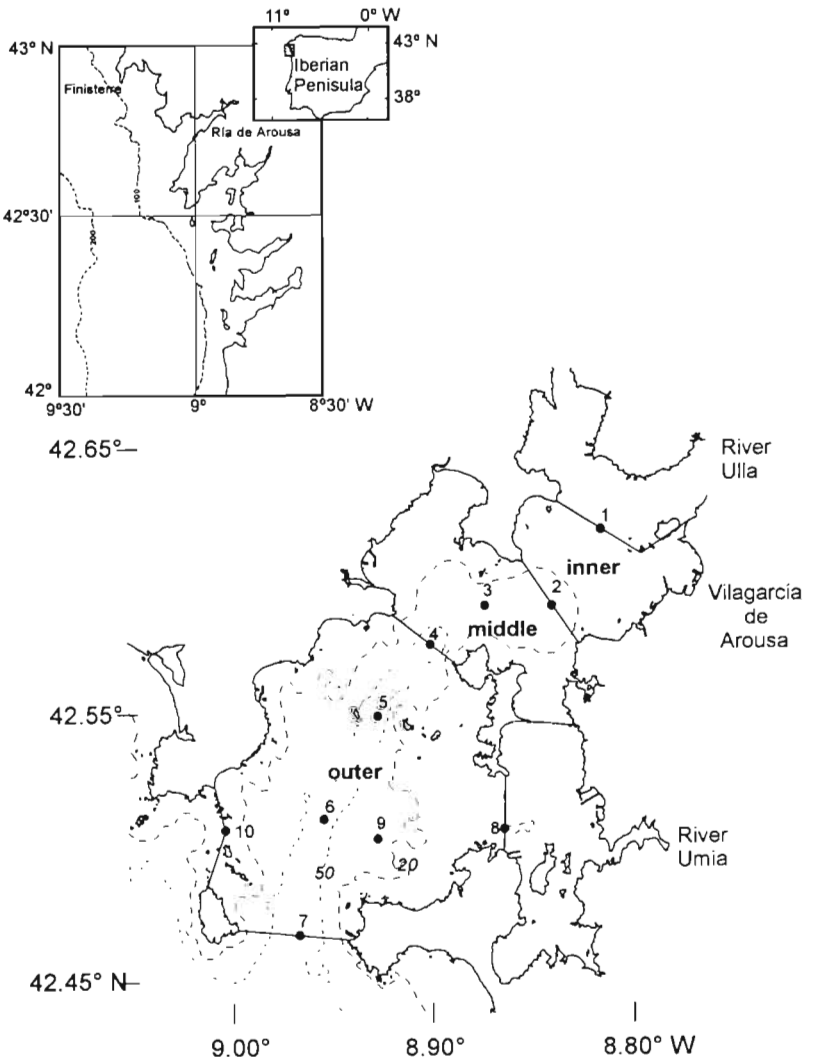

Fig. 1 The Ría de Arousa (NW Spain) survey area, with 20 and 50 m isobaths. Sampling stations are shown. The Ría was divided into three 2-layer segments (inner, middle and outer) to obtain water flows and carbon species fluxes and net budgets with an improved 2-D box-model. See Table 2 for geometric characteristics of the boxes

Water flows: Our 2-D non-stationary mass-heat weighted box model for calculating water flows has been extensively described by Rosón et al. (1997). The inputs to the model are the following: (1) the profiles of salinity and temperature at the 10 sampling sites; (2) the river flow (R), (3) the rainfall (P); (4) the evaporation (E) and the heat exchange flux across the sea surface (H), which were calculated with the empirical formulae obtained by Otto (1975) for the Ría; and (5) the geometry of the Ría (surface and cross-sectional areas and volumes), obtained from accurate charts published by the Spanish Instituto Geográfico de la Marina. The outputs from the model are the following (Fig. 3a): the hydrological balance ($R + P - E$), the upper (Q_X) and lower (Q_{X0}) horizontal convective flows, the vertical

Table 2. Geometric characteristics of the inner, middle and outer segments of the Ría de Arousa as defined in this study

Box	Volume ($\times 10^{-3}$ km^3) Total	Upper	Lower	Surface area (km^2)	Length (km)	Average depth (m)
Inner	229	119	110	22.5	3.4	10
Middle	785	392	393	42.1	5.7	19
Outer	3189	1428	1761	117.8	16.5	27

convective (Q_Z) and diffusive (M_Z) flows, and the 'boundary movement' ($Q_E = dV/dt$). Q_E is due to changes over time in the layer's volume (V) associated to the net upward displacement of the boundary between the upper and lower layer. Three 2-layered boxes have been considered: inner, middle and outer part of the Ría de Arousa (Fig. 1, Table 2).

Fluxes of carbon species: The flux of any carbon species (F_{Q_i}) transported by a convective water flow (Q_i) is the product of flow times concentration (C_i): $F_{Q_i} = Q_i \cdot C_i$. The river flux is $F_R = R \cdot C_R$, with C_R the concentration in the river flow. The vertical diffusive flux is $D = M_Z \cdot (C_L - C_U)$, where C_L and C_U are the respective concentrations in the upper and lower layer. The 'boundary movement' flux is $F_E = C \cdot dV/dt$. Concentrations are given in mol m^{-3}, flows in m^3 s^{-1} and fluxes in mol s^{-1}.

The CO_2 flux across the seawater-air interface (F_{CO_2}, in mol s^{-1}) was calculated with the classical formula:

$$F_{CO_2} = k\, S_{CO_2}\, (pCO_2 - pCO_{2_{ATM}})\, A \qquad (1)$$

where k (in m s^{-1}) is the piston velocity; S_{CO_2} (in mol m^{-3} µatm^{-1}) is the solubility of CO_2 in seawater; pCO_2 and $pCO_{2_{ATM}}$ (µatm) are the partial pressure of CO_2 at the sea surface and in the atmosphere, respectively; and A (m^2) is the surface area of the box (Table 2). A constant $pCO_{2_{ATM}}$ of 348 µatm was used as the average level during 1989 (Chipman et al. 1993). k was calculated by the equations of Woolf & Thorpe (1991) for smooth and rough water regimes. k depends on the wind speed 10 m above the sea surface. Analytical errors of pH (±0.005; Pérez & Fraga 1987a) and alkalinity (±2 µmol kg^{-1}; Pérez & Fraga 1987b) produce an error of ±7 µatm in the calculated pCO_2, whereas an error of ±1 m s^{-1} in wind velocity introduces an error of 15% in k. Finally, considering a $pCO_{2_{ATM}}$ variability during the study period of about ±3 µatm (Millero & Sohn 1992), the total error in F_{CO_2} is ~35%, since the average $pCO_2 - pCO_{2_{ATM}}$ was 50 µatm. These random errors do not affect either the temporal trend or the spatial differences of F_{CO_2} in the Ría during the selected periods.

Net budget of carbon species: The net budget (inputs minus outputs, $i - o$, in mol s^{-1}) of any carbon species in a box for any day sampled results from accumulation, $\partial(C \cdot V)/\partial t$, and biogeochemical processes, δC (positive: production; negative: consumption):

$$i - o = \frac{\partial(C \cdot V)}{\partial t} - \delta C = \sum_i F_{Q_i} + F_R - F_{CO_2} \qquad (2)$$

The net budget averaged between surveys $j - 1$ and j ($I - O$, in mol s^{-1}) can be obtained by integration of Eq. (2):

$$I - O = V \frac{C_{t_j} - C_{t_{j-1}}}{t_j - t_{j-1}} - \Delta C = \frac{\int_{t_{j-1}}^{t_j} \left(\sum_i F_{Q_i} + F_R - F_{CO_2} \right)}{t_j - t_{j-1}} \qquad (3)$$

where ΔC is the average δC between t_{j-1} and t_j. Average F_{Q_i} and F_R between t_{j-1} and t_j have been calculated assuming a linear change from t_{j-1} to t_j of (1) salinity, temperature, $R + P - E$, H and V for calculating water flows and (2) C, C_i and C_R for calculating fluxes. See Álvarez-Salgado et al. (1996a) and Rosón et al. (1997) for details.

A carbon budget for the upper layer would require the inward and outward horizontal convective fluxes (F_{Q_i}), the 3 vertical fluxes (F_Z, F_E and D) and F_{CO_2} to be considered. Finally, the budget for the lower layer can be obtained by subtracting the budget of the upper layer from the budget of the box.

The net budgets of TIC (ΔTIC) and TA (ΔTA) were obtained by solution of Eq. (3) for TIC and TA, respectively. TA and TIC, which depend specifically on salinity, needed correction since the net salinity budget (i.e. ΔS) was slightly different from zero in the mass-heat weighed box model (Rosón et al. 1997):

$$\Delta TA' = \Delta TA - 65.7 \cdot \Delta S \qquad (4)$$

$$\Delta TIC' = \Delta TIC - 60.0 \cdot \Delta S \qquad (5)$$

where the specific TA (65.7 µmol kg^{-1} pss^{-1}) and TIC (60.0 µmol kg^{-1} pss^{-1}) were the average of all samples collected in the study period (n = 2565).

Two biogeochemical processes contributed to ΔTIC': (1) NCP, i.e. the gross primary production minus the respiration of autotrophs and all heterotrophs (Platt et al. 1989), and (2) net calcium carbonate fixation ($\Delta CaCO_3$) to form calcareous structures. For oceanic waters $\Delta CaCO_3$ can be estimated from the following equation described by Broecker & Peng (1982):

$$\Delta CaCO_3 = -1/2 \cdot (\Delta TA' + \Delta NO_3^-) \qquad (6)$$

where ΔNO_3^- is the net budget of nitrate, because TA decreases 1 mole per mole of nitrate used during the synthesis of marine phytoplankton cells. In coastal and estuarine waters the influence of nitrite and ammonium have to be considered as well (Fraga et al. 1992):

$$\Delta CaCO_3 = -1/2 \cdot (\Delta TA' + \Delta NO_3^- + 0.45 \cdot \Delta NO_2^- - \Delta NH_4^+) \qquad (7)$$

TA increases 1 mole per mole of ammonium and increases 0.45 moles per mole of nitrite consumed, because ~45 % of the initial NO_2^- remain dissociated at pH = 4.4, since the dissociation constant of NO_2H is 4.4×10^{-5} (S = 35, t = 20°C; Spencer 1975). Finally, NCP can be calculated by subtracting $\Delta CaCO_3$ (Eq. 7) from $-\Delta TIC'$ (Eq. 5). Note that NCP and $\Delta TIC'$ have opposite signs.

The immediate fate of TIC trapped by NCP is the synthesis of particulate (ΔPOC) and dissolved (ΔDOC) organic carbon, and the deposition of organic carbon to the sediment (W_C):

$$NCP = \Delta POC + \Delta DOC + W_C \quad (8)$$

The particulate organic carbon budget (ΔPOC) is obtained by solving Eq. (5) for POC. W_C is estimated from:

$$W_C = W_P \cdot (POC/PTP) = -(\Delta PTP + \Delta DIP) \cdot (POC/PTP) \quad (9)$$

where W_P is the bottom deposition of particulate total phosphorus; ΔDIP and ΔPTP are the budgets for dissolved inorganic phosphorus and particulate total phosphorus, respectively (Álvarez-Salgado et al. 1996a); and POC/PTP is the particulate organic carbon to particulate total phosphorus ratio. The equality on Eq. (9) is consistent with the negligible dissolved organic phosphorus concentration in the Rías Baixas (Ríos 1992, Prego 1993a). W_C also accounts for the net carbon uptake by macrophytes and the removal of POC by large herbivores, mainly hanging mussels (10.4 g C m^{-2} yr^{-1} or 29 mg C m^{-2} d^{-1}; Álvarez-Salgado et al. 1996a). Since DOC was not measured at the time of survey, ΔDOC was estimated as the amount of carbon required to balance the carbon budget in Eq. (8).

RESULTS

Time course of fluxes and budgets of carbon species in the middle box

CO_2 exchange fluxes across the seawater-air interface (F_{CO_2}) in the middle segment of the Ría (Fig. 2a)

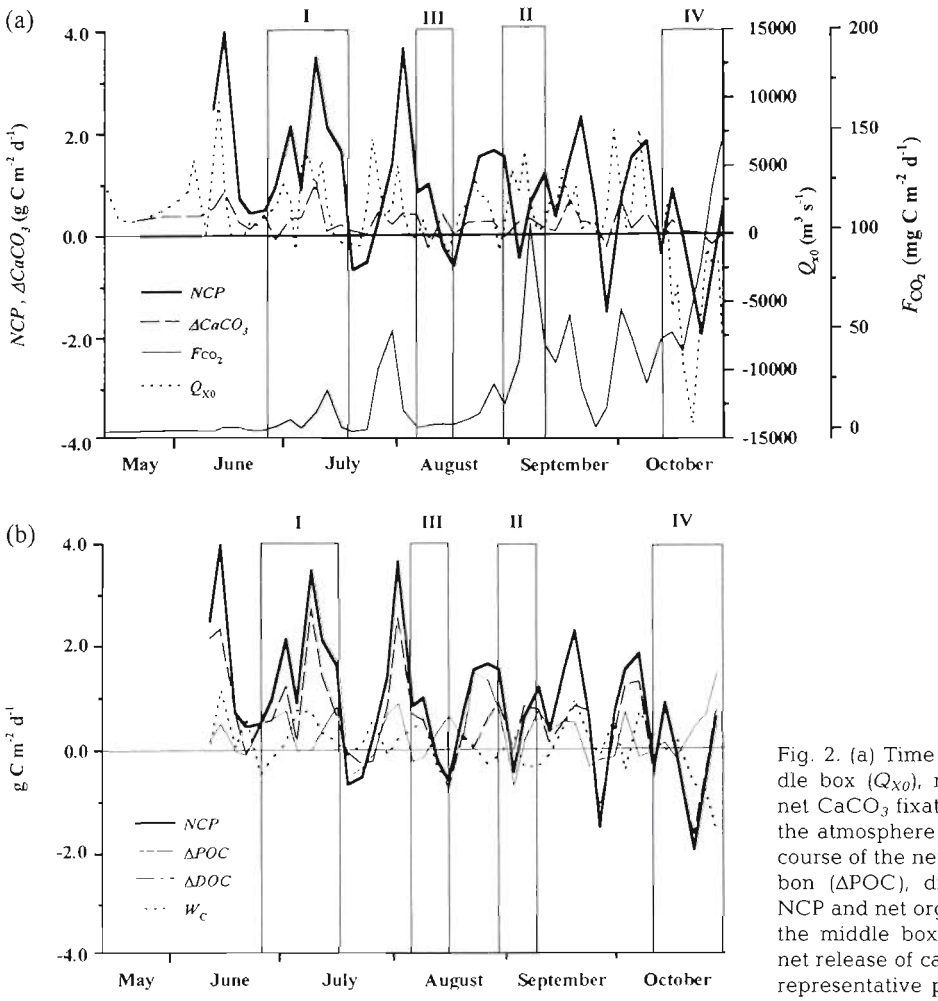

Fig. 2. (a) Time course of inward flow to the middle box (Q_{X0}), net community production (NCP), net $CaCO_3$ fixation ($\Delta CaCO_3$) and net CO_2 flux to the atmosphere (F_{CO_2}) in the middle box. (b) Time course of the net budget of particulate organic carbon (ΔPOC), dissolved organic carbon (ΔDOC), NCP and net organic carbon sedimentation (W_C) in the middle box. Negative values of W_C indicate net release of carbon from the sediments. I to IV: 4 representative periods of hydrographic variability

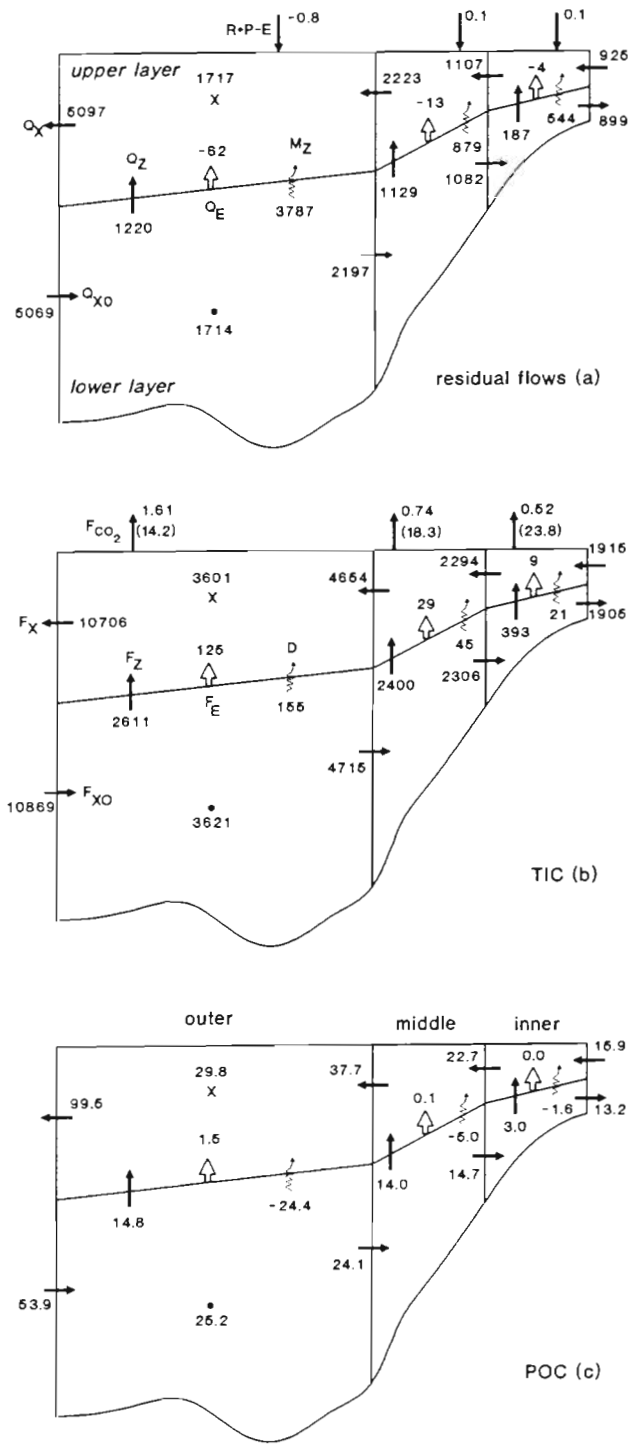

Fig. 3. (a) Average residual flows; (b) total inorganic carbon (TIC) fluxes; and (c) particulate organic carbon (POC) fluxes for the inner, middle and outer boxes over the upwelling season (June 8 to October 13, 1989). Q_X, Q_{X0}, Q_Z, Q_E, M_Z and $R + P - E$ in $m^3 s^{-1}$; TIC and POC fluxes in mol s^{-1}. Numbers in parentheses are F_{CO_2} in mg C m^{-2} d^{-1}

were negligible in the beginning of the study period (–0.2 mg C m^{-2} d^{-1}, average from May 11 to June 11). Thereafter, the Ría acted as a net source of CO_2 to the atmosphere (+22 mg C m^{-2} d^{-1}, average from June 11 to October 30). Relative maxima of +104 (September 7) and +136 mg C m^{-2} d^{-1} (October 27) coincided with periods of strong upwelling (period II) and autumn downwelling (period IV), respectively. Conversely, F_{CO_2} was low during periods of moderate upwelling (period I) and upwelling relaxation (period III).

Six major NCP maxima were observed during the study period, which ranged from 1.6 to 3.8 g C m^{-2} d^{-1} (Fig. 2a). These maxima were observed ~1 survey (3 to 4 d) after the residual current peaks ($Q_{X0} > 2.0 \times 10^3$ m^3 s^{-1}) that Rosón et al. (1997) associated with upwelling events. The magnitude of the NCP maxima was attenuated during the upwelling season. Upwelling period I coincided with 2 NCP maxima, whereas NCP decreased dramatically during upwelling period II. Low net production or even net carbon regeneration (between +0.5 and –1.5 g C m^{-2} d^{-1}) occurred with minimum values of Q_{X0}, associated with non-wind-forced conditions. These NCP minima occurred ~1 wk after the NCP maxima. Relaxation period III resulted in a dramatic decrease in NCP down to –0.6 g C m^{-2} d^{-1}. Finally, during downwelling period IV, residual circulation was strongly reversed (Q_{X0} up to -8.0×10^3 m^3 s^{-1}) and NCP became negative (up to –2.0 g C m^{-2} d^{-1}), indicating that carbon regeneration largely exceeded production.

NCP and $\Delta CaCO_3$ peaks were almost coincident in time (Fig. 2a). Although the daily values of $\Delta CaCO_3$ were much lower than NCP, $\Delta CaCO_3$ represented ~29% of NCP in the middle segment average over the upwelling season (June 8 to October 13). This percentage was large because calcium carbonate fixation ($\Delta CaCO_3 > 0$) occurred under any hydrographic circumstance, whereas NCP is reduced during relaxation periods. Following Eq. (8), NCP redistributed in the 3 carbon pools (ΔPOC, ΔDOC and W_C) as shown in Fig. 2b. During the upwelling season 28% of NCP was transformed to suspended POC which were exported to the shelf. Another 17% was deposited to the sediment in the Ría, whereas the remaining 55% was assumed to be exported as DOC (see Table 4) in order to balance the carbon budget.

Spatial differences along the embayment

Average upwelling season

The average Bakun's Upwelling Index I_W (a rough estimate of the volume of water upwelled per km of coast) for the upwelling season (June 8 to October 13) was 486 m^3 s^{-1} km^{-1} (Rosón et al. 1995). I_W contrasted

Table 3. Averaged residence times (in days) estimated from the geometric characteristics of each box and the whole Ría (Table 1) for the whole upwelling season and the selected periods

Period	From	To	Inner	Middle	Outer	Ría
Upwelling season	12 May	13 Oct	1.3	2.7	4.1	6.3
Upwelling following high stratification (I)	26 Jun	17 Jul	1.3	2.3	3.7	6.1
Upwelling following low stratification (II)	31 Aug	11 Sep	0.9	2.0	2.7	4.1
Upwelling relaxation (III)	07 Jul	17 Jul	4.5	29.9	11.2	13.5
Autumn downwelling (IV)	13 Oct	30 Oct	4.1	1.7	2.1	3.7

with the limited volumes of the rivers Ulla (925–899 = 26 $m^3 s^{-1}$) and Umia (1717 – 1714 = 3 $m^3 s^{-1}$) (Fig. 3a). In addition, $R + P - E$ in the 3 study boxes is negligible since R was very low in the limited catchment area of the boxes (Rosón et al. 1991). Water flows intensified along the main axis of the Ría (Fig. 3a), as the size of lateral sections increases oceanwards (Table 2). However, the middle box differed from the other in the following manner: in the inner and outer boxes the vertical water exchange was dominated by turbulent diffusion ($M_Z/Q_Z \approx 3$), whereas in the middle box advection prevailed ($M_Z/Q_Z \approx 0.8$). Note the steep change of bathymetry in the middle box, which enhances the response of circulation to upwelling (Álvarez-Salgado et al. 1996a). The average residence time was 6.3 d for the whole Ría (Table 3).

The major TIC input to the upper layer of the inner and outer boxes was by horizontal advection (Fig. 3b). The ratios between horizontal and Σ vertical fluxes were 4.5 and 2.9, respectively. In contrast, in the middle box the ratio was 0.9, i.e. favourable to the vertical flux. Vertical advection (F_Z) represented >90% of the TIC vertical flux ($F_Z + F_E + D$) into the upper layer in the 3 study boxes. The average CO_2 flux across the seawater-air interface (F_{CO_2}) was +16.3 mg C $m^{-2} d^{-1}$ during the upwelling season (Fig. 3b). F_{CO_2} per unit of surface area increased from the outer to the inner box.

The oceanward POC horizontal fluxes from the upper layer were higher than the coastward POC horizontal flux to the lower layer of any box (Fig. 3c), indicating a net export of POC to the shelf during the upwelling season. The difference increased from the inner to the outer box, where the average net POC export to the shelf was 45.6 mol s^{-1} (= 99.5 – 53.9). In contrast to the TIC vertical flux, vertical diffusive fluxes of POC were downwards, since $C_L - C_U$ is >0 for TIC but <0 for POC. In the inner and middle boxes the total vertical flux of POC was upwards (from the light-limited lower layer to the nutrient-limited upper layer), because the advective (F_Z) and 'boundary movement' (F_E) fluxes were greater than the diffusive flux (D). However, in the outer box a net downward flux of –8.1 mol C s^{-1} took place.

Biogeochemical processes trapped –0.95 g C $m^{-2} d^{-1}$ (ΔTIC') within the Ría during the upwelling season (Table 4). The middle segment was the most efficient trap (–1.2 g C $m^{-2} d^{-1}$), whereas in the inner and outer boxes ΔTIC' was ~30% lower than in the middle box. Calcium carbonate fixation ($\Delta CaCO_3$) and NCP contributed 12 and 88% to ΔTIC', respectively. ΔPOC in the Ría was ~30% of NCP during the upwelling season. Carbon removal from the water column by organic matter deposition and $CaCO_3$ fixation ($W_C + \Delta CaCO_3$) was 0.25 g C $m^{-2} d^{-1}$ in the Ría, 55% as organic carbon (W_C) and 45% as inorganic carbon ($\Delta CaCO_3$). In the outer box, the organic carbon represents ~81% of $W_C + \Delta CaCO_3$, whereas, in the middle box, the inorganic carbon became dominant and represented as much as 62% of the total carbon removal. In the inner box, net carbon removal occurred only by $CaCO_3$ fixation, whereas organic carbon resuspension took place ($W_C < 0$; Table 4).

Period I. Upwelling after high stratification

Period I coincided with high river volumes (average 52 $m^3 s^{-1}$) and moderate upwelling (average I_W = 734 $m^3 s^{-1} km^{-1}$), which was not able to erode the pycnocline (Álvarez-Salgado et al. 1996b). During this period, residence times (Table 3) in all boxes are comparable to those averaged over the upwelling season (Fig. 3a). Conversely, diffusive flows (M_Z) were less important in the vertical circulation because of stratification. M_Z/Q_Z was ~0.7 in the inner and outer segment, and as low as ~0.3 in the middle box.

The horizontal water flows in the middle and outer boxes were higher during period I than during the average upwelling season, which increased the horizontal TIC fluxes by more than 20% (Fig. 4b). The vertical transport of TIC was also dominated by advection and represented >93% of the total vertical exchange in all boxes. The CO_2 released to the atmosphere (+5.7 mg C $m^{-2} d^{-1}$) was ⅓ of the average flux of CO_2 during the upwelling season. F_{CO_2} were 70 and 14% larger in the inner and middle segments, respectively, than in the outer box.

Average horizontal POC fluxes in the outer box during period I (Fig. 4c) were ~47% higher than

Table 4. Net TIC' budget (ΔTIC'), C-based net community production (NCP), net calcium carbonate formation ($\Delta CaCO_3$), net POC budget (ΔPOC), and net POC deposition (W_C) for the whole Ría de Arousa and for the inner, middle and outer boxes during the whole upwelling season and the 4 periods studied. Values in g C m^{-2} d^{-1}, obtained from the values in mol s^{-1} multiplied by $1.037A^{-1}$, with A (surface area of the box) in km^2. Positive: production; negative: consumption

Box	ΔTIC'	NCP	$\Delta CaCO_3$	ΔPOC	W_C
Upwelling season					
Inner	−0.87	0.68	0.19	0.24	−0.10
Middle	−1.21	0.94	0.27	0.14	0.17
Outer	−0.87	0.83	0.04	0.27	0.17
Ría	−0.95	0.84	0.11	0.24	0.14
Upwelling after high stratification (I)					
Inner	−1.05	0.76	0.29	0.18	−0.06
Middle	−2.28	1.92	0.36	0.40	0.33
Outer	−1.56	1.48	0.08	0.40	0.29
Ría	−1.66	1.49	0.17	0.37	0.26
Upwelling after low stratification (II)					
Inner	−0.69	0.51	0.18	0.37	−0.44
Middle	−0.45	0.23	0.22	−0.15	−0.11
Outer	0.15	−0.20	0.05	0.03	−0.36
Ría	−0.10	−0.01	0.11	0.03	−0.31
Upwelling relaxation (III)					
Inner	−0.47	0.34	0.13	−0.04	−0.03
Middle	0.19	−0.27	0.08	−0.03	−0.13
Outer	0.31	−0.36	0.05	−0.18	0.11
Ría	0.18	−0.25	0.07	−0.13	0.04
Autumn downwelling (IV)					
Inner	0.21	−0.25	0.04	−0.03	−0.05
Middle	1.10	−1.13	0.03	−0.21	−0.59
Outer	0.26	−0.58	0.32	−0.50	−0.60
Ría	0.44	−0.66	0.22	−0.38	−0.53

those obtained during the average upwelling season (Fig. 3c). However, the net POC export to the shelf of 54.2 mol s^{-1} (= 145.9 − 91.7) was only ~20% higher. Advective POC transport from the light-limited lower layer to the nutrient-limited upper layer was >4-fold higher than the downwards diffusive transport in the 3 segments, as a consequence of stratification.

During period I, TIC trapped into the Ría by biogeochemical processes was −1.7 g C m^{-2} d^{-1}, i.e. 75% greater than during the average upwelling season. The most efficient segment was again the middle one (−2.3 g C m^{-2} d^{-1}). Only 10% of ΔTIC' was transformed to $CaCO_3$ in the Ría. POC production was ~54% higher than during the upwelling season. Total carbon removal (W_C + $\Delta CaCO_3$) reached its maximum value in the 4 study periods (+0.42 g C m^{-2} d^{-1}, Table 4), 60% of this was as POC deposited on the bottom. The contribution of W_C clearly diminished coastwards, and was 80 and 50% in the outer and middle segments, respectively. Conversely, in the inner box, net carbon release from the sediments was observed, which seemed to be a recurrent pattern throughout the upwelling season (Table 4).

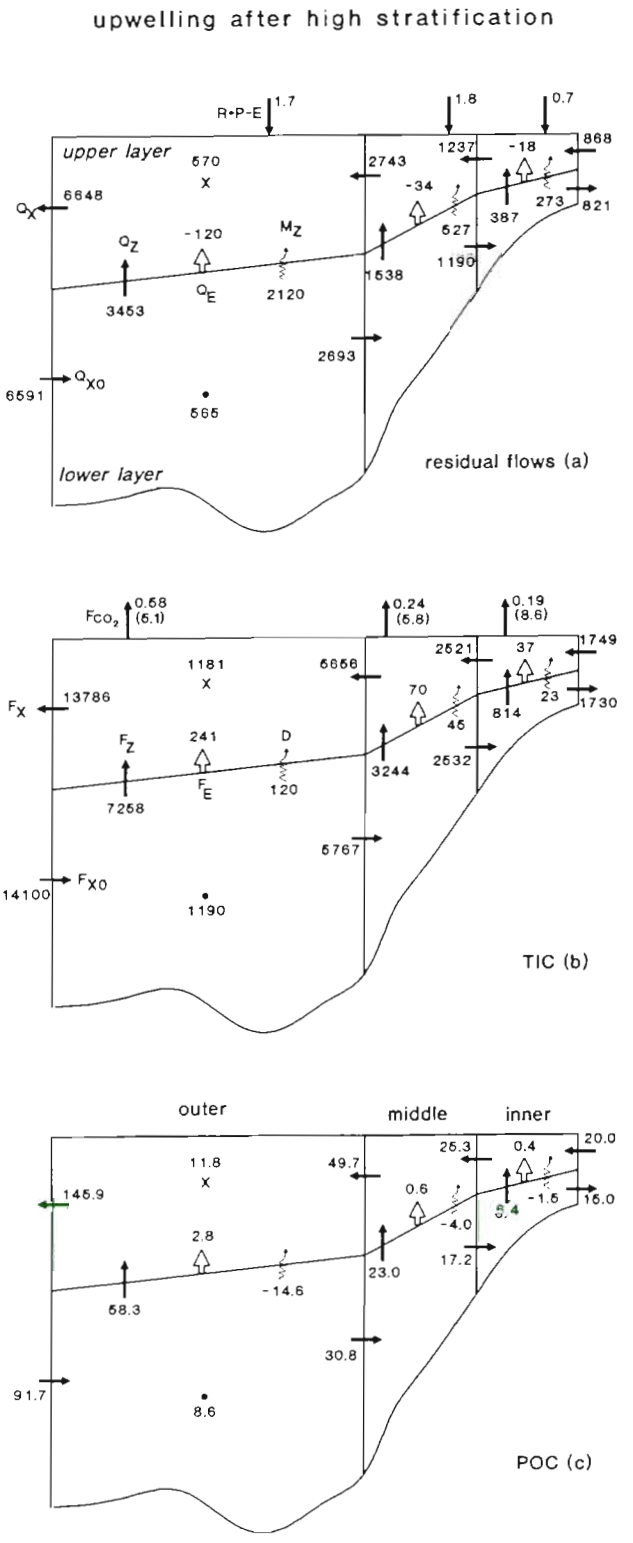

Fig. 4. (a) Average residual flows; (b) total inorganic carbon (TIC) fluxes; and (c) particulate organic carbon (POC) fluxes for the inner, middle and outer boxes for the upwelling after high stratification period (June 26 to July 17, 1989). Units as in Fig. 3

Period II. Upwelling after low stratification

The low river flows (average 12 $m^3 s^{-1}$) and a strong upwelling pulse (average I_W = 1242 $m^3 s^{-1} km^{-1}$) during this period forced intense positive circulation in the whole Ría (Fig 5a). Horizontal flows in the outer box increased by 86% compared to the average upwelling season. The increase was up to 4-fold in the convective vertical flow, and vertical diffusion was also enhanced by ~40%. The ratio M_Z/Q_Z (~1.2 for the whole Ría) was favourable to diffusion because of the absence of a marked pycnocline. Residence times were the shortest observed during the upwelling season in all boxes (~4 d for the entire Ría, Table 3).

As a result of the vigorous residual circulation, TIC fluxes (Fig. 5b) were also amplified compared to the average upwelling season (Fig. 3b). The absence of stratification allowed the CO_2-rich subsurface water to reach the surface. Thus, average F_{CO_2} in period II was +48 mg C $m^{-2} d^{-1}$, ~3-fold the average flux during the upwelling season. F_{CO_2} increased towards the river mouth.

POC fluxes during period II (Fig. 5c) were much higher than during the average upwelling season (Fig. 3c). They were similar to period I (Fig. 4c); 54.5 mol s^{-1} of POC (= 155.2 – 100.7) were exported to the adjacent shelf during this period. However, the only segment where significant POC production (ΔPOC) occurred was the inner box (+0.37 g C $m^{-2} d^{-1}$). Thus, POC exported to the shelf during this period did not result from *in situ* production, but from POC accumulated in the Ría.

The whole Ría trapped –0.1 g C $m^{-2} d^{-1}$, all as $CaCO_3$, since the average NCP was negligible (Table 4). NCP strongly decreased oceanwards, with net carbon regeneration in the outer box. Net carbon release from the sediments occurred during period II (W_C = –0.31 g C $m^{-2} d^{-1}$). Concurrently, $CaCO_3$ was formed throughout the Ría at the same rate as in the average upwelling season (+0.11 g C $m^{-2} d^{-1}$). This occurred mainly in the inner and middle boxes (about +0.20 g C $m^{-2} d^{-1}$).

Period III. Upwelling relaxation

Horizontal convective flows under non-wind-forced conditions (average I_W = 171 $m^3 s^{-1} km^{-1}$) became weak (–1200 < Q_X < 400 $m^3 s^{-1}$); reversed in the outer Ría but positive in the inner box (Fig. 6a). Residence times were the longest observed during the entire study period (Table 3), being 30 d in the middle segment where the convergence of the 2 opposite flows occurred. Vertical convective flows were downward in the 3 segments. TIC fluxes (Fig. 6b) also showed a decrease during this period. F_{CO_2} was low all over the

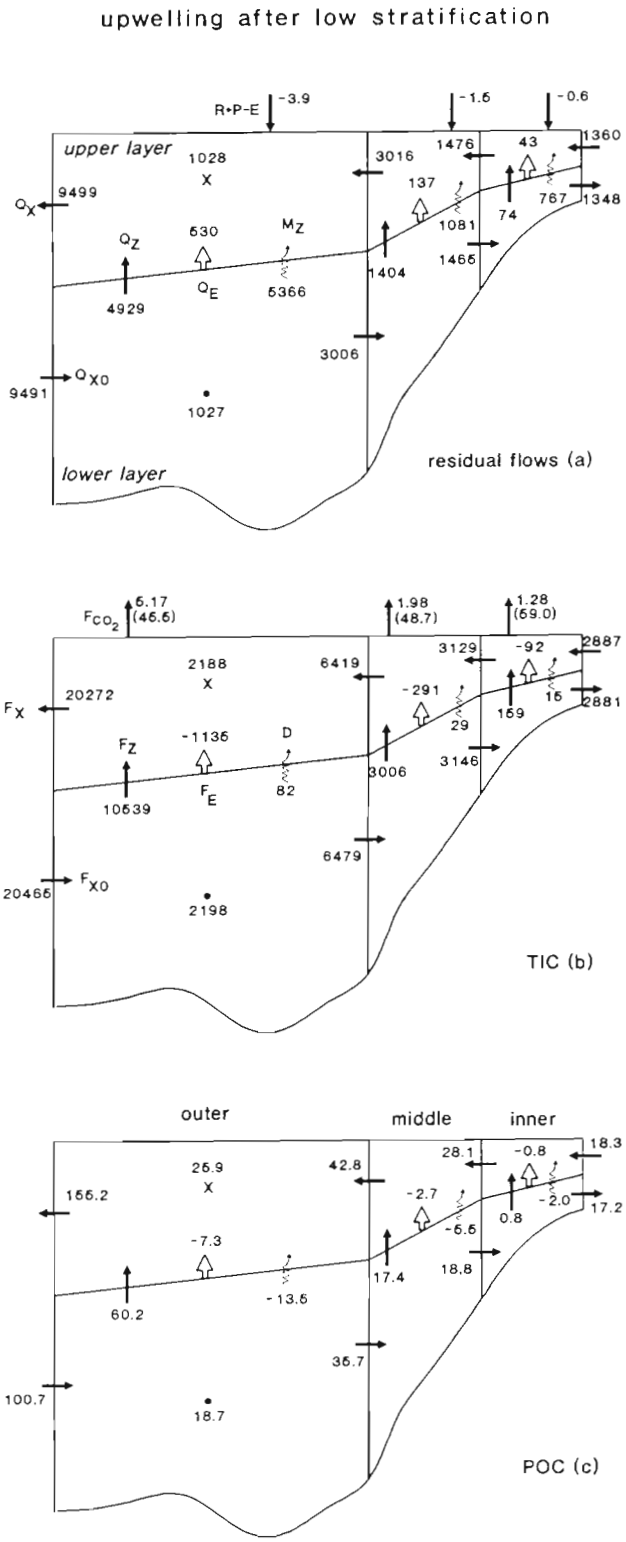

Fig. 5. (a) Average residual flows; (b) total inorganic carbon (TIC) fluxes; and (c) particulate organic carbon (POC) fluxes for the inner, middle and outer boxes for the upwelling after low stratification period (August 31 to September 11, 1989). Units as in Fig. 3

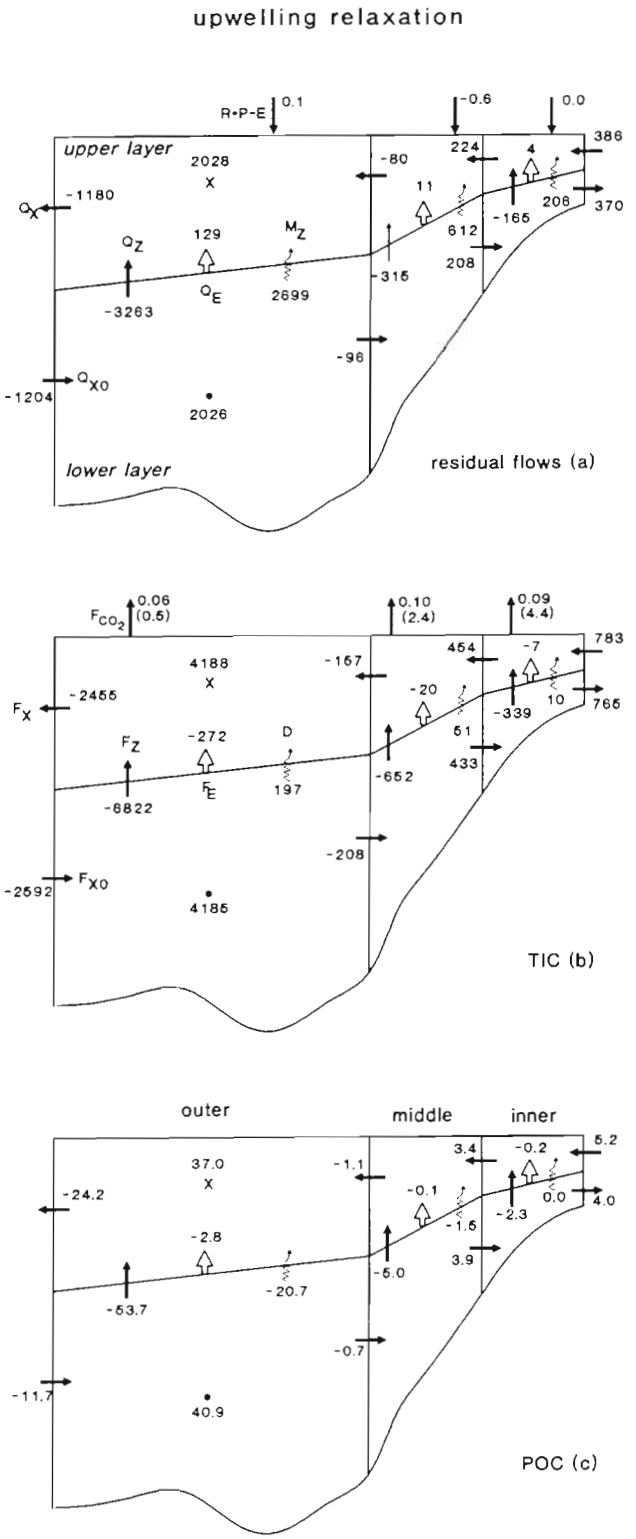

Fig. 6. (a) Average residual flows; (b) total inorganic carbon (TIC) fluxes; and (c) particulate organic carbon (POC) fluxes for the inner, middle and outer boxes for the upwelling relaxation period (August 7 to 17, 1989). Units as in Fig. 3

Fig. 7 (a) Average residual flows; (b) total inorganic carbon (TIC) fluxes; and (c) particulate organic carbon (POC) fluxes for the inner, middle and outer boxes for the autumn downwelling period (October 13 to 30, 1989). Units as in Fig. 3

Ría (<5 mg C m^{-2} d^{-1}), compared with exchange fluxes during wind-forced periods. POC fluxes also underwent a reduction (Fig. 6c), compared to the average upwelling season. A net entry of 12.5 mol s^{-1} of POC from the shelf occurred during this period. There was a net downward transport of POC from the upper to the lower layer mediated by F_E, F_Z and D, with vertical advection being dominant.

The pattern of ΔTIC' was also opposite to those observed under upwelling conditions (Table 4). Although net consumption of TIC occurred in the inner box (−0.47 g C m^{-2} d^{-1}), the Ría acted as a TIC source a (+0.18 g C m^{-2} d^{-1}), because of net TIC regeneration in the middle and outer boxes. Net consumption of POC occurred in the whole Ría (ΔPOC = −0.13 g C m^{-2} d^{-1}), but mainly in the outer box. Net organic carbon removal by deposition and $CaCO_3$ fixation was +0.11 g C m^{-2} d^{-1} during this period, less than half the average value for the upwelling season. This low value was associated with net carbon resuspension in the inner and middle boxes (W_C <0, Table 4), whereas $\Delta CaCO_3$ was positive in the whole Ría.

Period IV. Autumn downwelling

Strong southerly winds (average I_W = −706 m^3 s^{-1} km^{-1}) provoked a reversal of residual circulation, characterised by intense horizontal and vertical convective flows (Fig. 7a). However, circulation was still positive in the innermost station. Residence times were short (<2 d) in the outer and middle segments compared to the other study periods (Table 3). Diffusive flows were important in the outer and inner segments (absolute value of M_Z/Q_Z > 0.9). However, the dominance of vertical advection due to the abrupt change of bathymetry was still observed in the middle box (absolute value of M_Z/Q_Z > 0.3).

The rapid water exchange between the different segments of the Ría provoked high TIC fluxes (Fig. 7b). The diffusive vertical transport of TIC was reduced, despite the strong diffusive flows. This indicates strong vertical homogenisation ($C_L \approx C_U$), as observed in the distributions presented by Rosón et al. (1995). The largest F_{CO_2} during the entire study period were observed during period IV (+55 mg C m^{-2} d^{-1}). Since the budget of inputs minus outputs ($I - O$) in the inner box was −5.48 mol s^{-1}, F_{CO_2} represented as much as 45% of the total TIC budget. Horizontal and vertical POC fluxes during period IV were also the highest of the entire study period (Fig. 7c). There was a net POC import of 67.8 mol s^{-1} from the shelf into the surface layer of the Ría. Vertical convection was the most important mechanism of downward transport of POC under these conditions.

TIC regeneration took place in the whole Ría (ΔTIC' = +0.44 g C m^{-2} d^{-1}). As maximum calcium carbonate fixation rates were observed during this period, organic carbon mineralization (NCP < 0) occurred at an average net rate of −0.66 g C m^{-2} d^{-1}. Both the oxidation of suspended POC and the net carbon release from the sediments contributed to the observed regeneration. The system was balanced with the net production of 0.25 g C m^{-2} d^{-1} of DOC.

DISCUSSION

Origin and fate of carbon trapped within the Ría

Average NCP in the Ría de Arousa during the upwelling season (0.84 g C m^{-2} d^{-1}) exceeded the average annual NCP (~0.14 to 0.33 g C m^{-2} d^{-1}) of the global coastal zone (Wollast 1991, 1993). Conversely, the value is similar to the annual mean of gross primary production proposed by Boynton et al. (1982) for upwelling areas (~0.82 g C m^{-2} d^{-1}). Our NCP value constitutes a very solid average, because it embraces all the possible contrasting hydrodynamic situations during the upwelling season. NCP in the middle box was comparable with the average value obtained by Moncoiffé et al. (1993) by the oxygen incubation method during the upwelling season of 1991 in the central portion of the adjacent Ría de Vigo (0.7 to 0.9 g C m^{-2} d^{-1}). The tendency of NCP to diminish during the study period (Fig. 2), which is associated with the progressive decrease of pH and increase of TIC and pCO_2 (Rosón et al. 1995) levels in the water column, were suggestive of increasing carbon regeneration in the Ría. These changes over time were associated with decreased insolation and daylength during the study period.

As much as 83% of NCP was organic carbon exported to the shelf. Following Álvarez-Salgado et al. (1996a), the ratio of net to gross primary production (f_{RATIO}) during the upwelling season is ~0.6. Therefore, organic matter export would represent ~50% of total production, which is much higher than the 15% export from the global coastal zone to the deep ocean (Wollast 1991, 1993). Wollast's calculations were mostly based on POC. It is important to note that POC export represents 15% of the total production in the Ría. So, our results show that consideration of DOC produced in the Ría is crucial for a realistic estimation of organic matter export in the study area. Conversely, 17% of NCP contributed to W_C. This number is much lower than the average deposition over the bottom of 32% of the total production proposed by Wollast (1991, 1993).

As $CaCO_3$ fixation was enhanced during upwelling conditions (NCP and $\Delta CaCO_3$ maxima were nearly

coincident), it seems that high production rates associated with upwelling pulses stimulate mussel growth and, therefore, calcium carbonate uptake. However, $CaCO_3$ fixation occurred almost all the time, even during periods of net carbon regeneration. This has also been observed by Frankignoulle & Gattuso (1993) in coral reefs. Annual production of mussels on hanging ropes (total wet weight) in the whole Ría de Arousa is ~1.2×10^5 metric tonnes (Tenore et al. 1982). Shells with ~90% $CaCO_3$ content (U. Labarta pers. comm.) represent ~35% of a commercial mussel's net weight (Andreu 1963). Therefore, the total amount of carbon removed from the water column to form mussel shells yielded an average daily value of ~68 mg C m^{-2} d^{-1}, i.e. 55% of the estimated $CaCO_3$ fixation rate in the Ría during the study period. The remaining 45% must correspond to $CaCO_3$ taken up by calcareous algae, other bivalve species (rock mussels, clams, oysters, cockles, etc.) and crustaceans.

Air-sea CO_2 exchange. The Ría de Arousa, a net source of CO_2 to the atmosphere

It seems contradictory that a highly productive system such as the Ría de Arousa is a source of CO_2 rather than a sink during late spring, summer and early autumn. A rough estimation of the influence of NCP and $\Delta CaCO_3$ in the time variation of surface pCO_2 in the middle box will cast some light on this intriguing point. We have chosen as initial conditions ($t = 0$) the average measured values of salinity, temperature, pH and alkalinity throughout the water column in the middle box during the entire study period to calculate the initial TIC and pCO_2. The effect of NCP and $\Delta CaCO_3$ on TIC and alkalinity changes can be calculated as (Gattuso et al. 1995):

$$(TIC)_t = (TIC)_{t=0} - \Delta CaCO_3 - NCP \quad (10)$$

$$(TA)_t = (TA)_{t=0} - 2\,\Delta CaCO_3 - \Delta NO_3 = (TA)_{t=0} - 2\,\Delta CaCO_3 - NCP/7.0 \quad (11)$$

Eq. (11) was derived from Eq. (6), because 90% of NCP was supported by nitrate in the middle segment (Álvarez-Salgado et al. 1996a). The slope of the correlation between the C- and N-based daily NCP rates, 7.0 ± 0.4 mol C mol N^{-1} ($r^2 = 0.78$), was used to convert from carbon to nitrogen units. By considering the average NCP and $\Delta CaCO_3$ over the upwelling season in the middle box (Table 4), mean daily changes of $(TIC)_t$ and $(TA)_t$ can be obtained. The mean daily change of pCO_2 can be derived by means of the carbonic system equations, being −8.2 ± 0.1 µatm d^{-1} (10 d average). Finally, actual surface pCO_2 is correlated with water-column-integrated pCO_2 changes ($r^2 = 0.72$), the slope being 1.1 ± 0.1. Consequently, the mean daily decrease in surface pCO_2 associated with the average NCP and $\Delta CaCO_3$ during the upwelling season in the middle box (Table 4) was −9.1 ± 0.2 µatm d^{-1}. As the mean residence time in the middle box was 2.7 d (Table 3), the expected average decrease of surface pCO_2 should be ~25 µatm. Since $(pCO_2)_{t=0}$ was 404 µatm, the final pCO_2 would be 379 µatm, which is 31 µatm above $pCO_{2_{ATM}}$. The residence time required to equilibrate the middle segment of the Ría with the atmosphere should be ~6.0 d.

$CaCO_3$ fixation increases pCO_2 in the Ría, since removal of CO_3^{2-} contributes to acidify the water column. Calculations can be made for the hypothetical situation in which $\Delta CaCO_3 \approx 0$. In this case, $\Delta pCO_2/\Delta t$ = −10.2 ± 0.2 µatm d^{-1} and surface pCO_2 after the residence time should be 376 µatm, i.e. only 3 µatm lower than before. So, the influence of $CaCO_3$ fixation by the intensive culture on mussel rafts on the behaviour of the Ría as a source of CO_2 is minor. Frankignoulle & Gattuso (1993) also found that $CaCO_3$ fixation in coral reefs have a minor impact on F_{CO_2}.

In light of this discussion, there are possibly 2 reasons to explain the observed behaviour. Firstly, very high initial pCO_2 levels in the source ENACW, which ages on the shelf (Álvarez-Salgado et al. 1993) and in the Ría. Secondly, short residence times which did not allow the phytoplankton community to reduce the pCO_2 levels below atmospheric values.

Changes in pH and temperature of surface water are the key variables affecting the variability of surface pCO_2. The variances of pH and temperature in the middle segment during the study period were ±0.06 and ±0.8°C, respectively. Their contribution to the variance of surface pCO_2 can be calculated using the equations of the carbonic system, being ±86 µatm for pH and ±30 µatm for temperature. The CO_2 fluxes across the sea surface, F_{CO_2} (Eq. 1), were also affected by wind speed, which had an observed variance of ±1.5 m s^{-1}. The average contributions of pH, temperature and wind speed to the total variance of F_{CO_2} are ±11, ±4 and ±13 mg C m^{-2} d^{-1}, respectively. Therefore, 39% of the total variance was due to 'biogeochemical' changes, 14% due to 'physical' changes and 47% due to 'kinetic' changes.

F_{CO_2} in the Ría de Arousa was opposite to those obtained by Prego (1993b; −6.6 mg C m^{-2} d^{-1}, average over 6 surveys in February to October 1986) and Álvarez (1996; −8.6 mg C m^{-2} d^{-1} averaged over the upwelling season of 1995) in the adjacent Ría de Vigo. As we have stated in the previous chapter, the NCP and f_{RATIO} were similar in both rías during the upwelling season (Álvarez-Salgado et al. 1996a, Moncoiffé et al. 1993). Source ENACW must be essentially the same too. Thus, the main difference between both rías has to be the residence times, being longer in the

Ría de Vigo than in the Ría de Arousa. In this sense, Ríos (1992) reported an average residence time of ~7 d in the central segment of the Ría de Vigo during the upwelling season of 1988. This value is much greater than the ~3 d obtained in the central Ría de Arousa and exceeds the ~6 d required for equilibration. Figueiras & Pazos (1991) also pointed out this important disparity in relation to the different selection of phytoplankton species in both ecosystems. However, this key issue needs a future process-orientated study, comparing both rías simultaneously.

F_{CO_2} decreased shelfwards during the upwelling season, following the decreasing pattern of surface pCO_2 levels along the main axis of the Ría which range from 445 ± 78 µatm at Stn 1 to 370 ± 48 µatm at Stn 7. Pérez et al. (in press) obtained average F_{CO_2} values of −16.8 and +3.2 mg C m^{-2} d^{-1} in shelf water off the rías during cruises in May 1993 (prevalence of southwesterly winds) and July 1994 (prevalence of northerly winds), respectively. The average F_{CO_2} value in the Ría de Arousa is comparable with other oceanic and coastal upwelling regions. Andrié et al. (1986) estimated an average F_{CO_2} of +12.6 mg C m^{-2} d^{-1} during 5 cruises to the Equatorial Atlantic. Values in the Equatorial Pacific are greater than in the Equatorial Atlantic, ranging from +16.9 to +58.6 mg C m^{-2} d^{-1} (Lefèvre et al. 1994, Ishii & Inoue 1995). F_{CO_2} is also high in the Peruvian coastal upwelling region, where Copin-Montégut & Raimbault (1994) observed surface pCO_2 levels as high as 1000 µatm in recently upwelled waters during winter 1991. Conversely, Simpson & Zirino (1980) have shown that upwelled water can rapidly become a sink for atmospheric CO_2 due to the high rates of production in this area. Finally, strong post-spring tides can carry cold and CO_2-rich waters to the surface, leading to very high F_{CO_2} values in the Gulf of California (average +100 mg C m^{-2} d^{-1}; Hidalgo-González et al. 1997).

Carbon biogeochemistry during the four contrasting periods

It is known that upwelling systems reach their maximum productivity under moderate winds (Huntsman & Barber 1977, Wroblewski & Hoffmann 1989), when long residence times allow phytoplankton adaptation to the new light and nutrient conditions. As a result, phytoplankton growth rates stimulated by the input of new nitrate exceeds cell 'washout'. Period I seems to be an example of this situation, when upwelling was not able to erode the pycnocline. The high NCP during this period indicates that light-adapted phytoplankton cells were able to grow fast and accumulate at the expense of the moderate input of new nutrients. Under circumstances of moderate upwelling, the pycnocline prevents the massive transport of pCO_2-rich, aged water to the surface. Thus, surface pCO_2 levels and CO_2 exchange fluxes are relatively low during this period: only 35% of the value during the average upwelling season.

However, stronger northerly winds (I_W > 1000 m^3 s^{-1} km^{-1}) can erode the pycnocline and deep water reaches the surface. Under circumstances of strong upwelling, phytoplankton in the photic layer is exported towards the shelf. It is replaced by slow-growing cells carried by the upward flowing deep water, which is not adapted to the high nutrient and light conditions (Zimmerman et al. 1987). This seems to be the situation observed during period II, when northerly winds were about twice as strong as during the average upwelling season. NCP was negative in the outer box, it reduced to ¼ of the averaged valuze for upwelling season in the middle box, and it was relatively high in the inner segment because it was protected against upwelling (Table 4). As the pCO_2-rich ENACW reached the surface, CO_2 fluxes to the atmosphere became as high as +48 mg C m^{-2} d^{-1} during this period. Although NCP increased coastwards, F_{CO_2} increased in the same direction because of the effect of the progressive CO_2 enrichment of ENACW entering the Ría and the reduced residence times (<1 d) in the inner box. Prego (1993b) also observed a strong F_{CO_2} peak of +53 mg C m^{-2} d^{-1} in the adjacent Ría de Vigo during a strong upwelling pulse.

When winds over the shelf relax after an upwelling event, the system returns slowly to the conditions previous to upwelling. Upwelled water moves downward to its original depth, provoking a reversal in estuarine circulation in the external part of the Ría. pCO_2-rich upwelled water is replaced by nutrient-depleted pCO_2-equilibrated shelf surface waters. In addition, vertical transport of nutrients to the upper layer under these flow conditions was prevented. Q_Z was negative (downwards) and M_Z was low because of the marked pycnocline and the upper layer became nutrient-limited (Álvarez-Salgado et al. 1996b). This was the situation during period III, characterised by slight regeneration in the outer and middle boxes and net production in the inner segment. Reduced CO_2 exchange fluxes across the sea surface during periods of prolonged relaxation were due to (1) the entry of shelf surface waters close to equilibrium of CO_2 with the atmosphere; (2) the very long residence times which favour equilibration of CO_2; and (3) the weak local winds, which lower the value of the piston velocity, k. F_{CO_2} increased coastwards due to organic carbon mineralization in outer and middle boxes. The same situation occurred in the Ría the Vigo during September 1986 (Prego 1992).

Transition from predominantly northerly to predominantly southerly winds usually occurs by September-

October (Wooster et al. 1976, Blanton et al. 1987). Strong reversal in estuarine circulation takes place, with the upwelled water being rapidly evacuated through the bottom of the Ría. This process favours sediment mobilization and high CO_2 (and NH_4^+; Álvarez-Salgado et al. 1996b) fluxes from the sediments to the water column. In addition, this is also the time of the intense autumn regeneration (Nogueira et al. 1997) and the concomitant massive increase of CO_2 in the water column. This was the situation during period IV, when the highest F_{CO_2} fluxes to the atmosphere were recorded (+55 mg C m^{-2} d^{-1} on average). Maximum fluxes occurred in the inner box, where carbon release from the sediments was minimal. However, there was an input of aged waters, because of the intense mineralization of the large population of macrophytes in the upper reaches of the estuary (Pérez et al. 1992). pCO_2 levels reached 622 µatm at Stn 1 on October 30. In addition to carbon regeneration, the advection of warm surface water from the shelf (average 15.2°C) and the strong local winds (average 6 m s^{-1}) enhanced F_{CO_2} fluxes.

SUMMARY AND CONCLUSIONS

Carbon biogeochemistry in the Ría de Arousa strongly depends on hydrodynamics, which is forced by wind stress over the shelf. Primary production during the upwelling season is not able to reduce the high pCO_2 levels in ENACW below the atmospheric levels, probably because the short residence times did not allow equilibration with the atmosphere. So, the Ría acts as a source of CO_2 to the atmosphere (+16.3 mg C m^{-2} d^{-1}). The effect of calcium carbonate fixation by mussels on hanging ropes did not significantly affect CO_2 exchange fluxes. Aging of source ENACW increased and residence time decreased coastwards. Consequently, CO_2 exchange fluxes per unit area from seawater to the atmosphere were twice as high in the inner as in the outer box. Under conditions of moderate upwelling, carbon uptake by the community of organisms within the Ría reached a maximum, and the CO_2 exchange fluxes reduced to ⅓ the average value during the upwelling season. During strong upwelling events, the pCO_2-rich ENACW reached the surface, which caused the highest CO_2 exchange fluxes over the upwelling period. Moderate NCP occurred only in the inner box, where the upwelling effects were reduced. Finally, under non-wind-forced conditions, ENACW in the Ría returned to the shelf and the nutrient-depleted CO_2-equilibrated shelf surface water occupied the Ría. CO_2 exchange fluxes were the lowest during the upwelling season. It is interesting to note that the inner Ría showed a particular behaviour throughout the upwelling season independent of the wind regime over the shelf; it was always productive (NCP > 0); and carbon release from the sediments occurred all the time (W_C < 0), contributing to an increase of pCO_2. In addition, $CaCO_3$ fixation occurred all the time and throughout the Ría during the upwelling season, although maximum rates coincided with maximum NCP peaks. Finally, carbon biogeochemistry was deeply affected by a strong autumn downwelling event. The high CO_2 exchange fluxes during this period, more than 3-fold the average during the upwelling season, were due to carbon regeneration throughout the Ría, with intense carbon release from the sediments.

Acknowledgements. The authors thank all the participants in the Galicia-X cruise from the Instituto de Investigacións Mariñas and the crew of the R/V 'Investigador S.', for their valuable help. We also thank Dr G. Tilstone and 4 anonymous reviewers for their valuable comments and criticisms. Support for this work came from C.I.C.Y.T grant number MAR88-0245 and funds from the Conselleria de Pesca da Xunta de Galicia. Fellowships from the Spanish M.E.C. have enable X.A.A.-S. and G.R. to carry out their Ph.D. theses as part of this project.

LITERATURE CITED

Álvarez M (1996) Flujos de CO_2 océano-atmósfera en un medio costero: control físico versus biológico. BSc thesis, University of Vigo

Álvarez-Salgado XA (1993) Mecanismos de transporte e balance bioxeoquímico do nitróxeno na Ría de Arousa. PhD thesis, University of Santiago de Compostela

Álvarez-Salgado XA, Rosón G, Pérez FF, Pazos Y (1993) Hydrographic variability off the Rías Baixas (NW Spain) during the upwelling season. J Geophys Res 98(C8): 14447–14455

Álvarez-Salgado XA, Rosón G, Pérez FF, Figueiras FG, Pazos Y (1996a) Nitrogen cycling in an estuarine upwelling system, the Ría de Arousa (NW Spain). I. Short-time-scale patterns of hydrodynamic and biogeochemical circulation. Mar Ecol Prog Ser 135:259–273

Álvarez-Salgado XA, Rosón G, Pérez FF, Figueiras FG, Ríos AF (1996b) Nitrogen cycling in an estuarine upwelling system, the Ría de Arousa (NW Spain). II. Spatial differences in the short-time-scale evolution of fluxes and net budgets. Mar Ecol Prog Ser 135:275–288

Álvarez-Salgado XA, Castro CG, Pérez FF, Fraga F (1997) Nutrient mineralization patterns in shelf waters of the NW Iberian upwelling system. Cont Shelf Res 17:1247–1270

Andreu B (1963) El mejillón como primera materia prima para la conserva. Información conservera 119:404–410

Andrié C, Oudot C, Genthon C, Merlivat L (1986) CO_2 fluxes in the tropical Atlantic during FOCAL cruises. J Geophys Res 91(C10):11741–11755

Bakun A (1973) Coastal upwelling indices, west coast of North America 1946–1971. NOAA technical report, NMFS-SSRF–671

Blanton JO, Tenore KR, de Castillejo FF, Atkinson LP, Schwing FB, Lavín A (1987) The relation of upwelling to mussel production in the rías on the western coast of Spain. J Mar Res 45:497–511

Boynton WR, Kemp WM, Keefe CW (1982) A comparative analysis of nutrients and other factors influencing estuarine phytoplankton production. In: Kennedy VS (ed) Estuarine comparisons. Academic Press, New York, p 69–90

Broecker WS, Peng TH (1982) Tracers in the sea. Eldigio Press, New York

Chipman DW, Marra J, Takahashi T (1993) Primary production at 47°N and 20°W in the North Atlantic Ocean: a comparison between de ^{14}C incubation method and the mixed layer carbon budget. Deep-Sea Res I 40:151–169

Copin-Montégut C, Raimbault P (1994) The Peruvian upwelling near 15°S in August 1986. Results of continuous measurements of physical and chemical properties between 0 and 200 m depth. Deep-Sea Res I 41:439–467

Doval MD, Álvarez-Salgado XA, Pérez FF (1997) Dissolved organic carbon in an coastal embayment affected by upwelling. Mar Ecol Prog Ser 157:21–37

Figueiras FG, Pazos Y (1991) Microplankton assemblages in three Rías Baixas (Vigo, Arosa and Muros, Spain) with a subsurface chlorophyll maximum: their relationships to hydrography. Mar Ecol Prog Ser 76:219–233

Fraga F, Pérez FF, Figueiras FG, Ríos AF (1992) Stoichiometric variations of N, P, C, and O_2 during a *Gymnodinium catenatum* red tide and their interpretation. Mar Ecol Prog Ser 87:123–134

Frankignoulle M, Gattuso JP (1993) Air sea CO_2 exchange in coastal ecosystems. In: Wollast R, Mackenzie FT, Chou L (eds) Interactions of C, N, P and S biogeochemical cycles and global change. NATO ASI Series 14, Springer-Verlag, Berlin, p 233–248

Gattuso JP, Pichon M, Frankignoulle M (1995) Biological control of air-sea CO_2 effect of photosynthetic and calcifying marine organisms and ecosystems. Mar Ecol Prog Ser 129: 307–312

Hidalgo-González RM, Álvarez-Borrego S, Zirino A (1997) Mixing in the region of midrift islands of the Gulf of California: effect on surface pCO_2. Cienc Mar 23:317–327

Huntsman SA, Barber RT (1977) Primary production off northwest Africa: the relationship to wind and nutrient conditions. Deep-Sea Res 24:25–33

Ishii M, Inoue HY (1995) Air-sea exchange in the central and western equatorial Pacific in 1990. Tellus 47B:447–460

Lefèvre N, Andrié C, Dandonneau Y, Reverdin G, Rodier M (1994) pCO_2, chemical properties, and estimated new production in the equatorial Pacific in January–March 1991. J Geophys Res 99(C6):12639–12654

Mehrbach C, Culberson CH, Hawley JE, Pytkowitcz RM (1973) Measurements of the apparent dissociation constants of carbonic acid in seawater at atmospheric pressure. Limnol Oceanogr 18:897–906

Middleburg JJ, Vlug T, Van der Nat FJWA (1993) Organic matter mineralization in marine systems. Global Planet Change 8:47–58

Millero FJ, Sohn ML (1992) Chemical oceanography. CRC Press Inc, Boca Raton

Moncoiffé G, Savidge G, Álvarez-Salgado XA, Figueiras FG (1993) Variability of surface planktonic community metabolism in response to coastal upwelling events in the Ría de Vigo (NW Spain). Int Counc Explor Sea Counc Meet Pap, ICES, Copenhagen

Nogueira E, Pérez FF, Ríos AF (1997) Seasonal patterns and long-term trends in an estuarine upwelling ecosystem (Ría de Vigo, NW Spain). Estuar Coast Shelf Sci 44:285–300

Otto L (1975) Oceanography of the Ría de Arousa (NW Spain). Konink Meteor Int Med Verlan No. 96. Leiden University

Pazos Y, Figueiras FG, Álvarez-Salgado XA, Rosón G (1995) The control of succession in red tide species in the Ría de Arousa (NW Spain) by upwelling and stability. In: Lassus P, Arzul G, Erad E, Gentien P, Marcaillou C (eds) Harmful algal blooms. Lavoisier, Intercept Ltd, Paris, p 645–650

Pérez FF, Álvarez-Salgado XA, Rosón G, Ríos AF (1992) Carbonic-calcium system, nutrients and total organic nitrogen in continental runoff to the Galician Rías Baixas, NW Spain. Oceanol Acta 15:595–602

Pérez FF, Fraga F (1987a) The pH measurements in seawater on NBS scale. Mar Chem 21:315–327

Pérez FF, Fraga F (1987b) A precise and rapid analytical procedure for alkalinity determinations. Mar Chem 21 169–182

Pérez FF, Ríos AF, Rosón G (in press) Air-sea exchange of carbon dioxide off Iberian Peninsula (East North Atlantic Ocean). J Mar Syst

Platt T, Harrison WG, Lewis MR, Li WKW, Sathyendranath S, Smith RE, Vezina AF (1989) Biological production of the oceans: the case for a consensus. Mar Ecol Prog Ser 52: 77–88

Prego R (1992) Flows and budgets of nutrient salts and organic carbon in relation to a red tide in the Ría of Vigo (NW Spain). Mar Ecol Prog Ser 79:289–302

Prego R (1993a) Biogeochemical pathways of phosphorus in a Galician Ría. Estuar Coast Shelf Sci 37:437–451

Prego R (1993b) General aspects of carbon biogeochemistry in the Ría of Vigo, northwestern Spain. Geochim Cosmochim Acta 57:2041–2052

Prego R, Fraga F (1992) A simple model to calculate the residual flows in a Spanish Ría. Hydrographic consequences in the Ría of Vigo. Estuar Coast Shelf Sci 34:603–615

Ríos AF (1992) El fitoplancton de la Ría de Vigo y sus condiciones ambientales. PhD thesis, University of Santiago de Compostela

Rosón G, Álvarez-Salgado XA, Pérez FF (1997) A non-stationary box-model to determine residual flows in a partially mixed estuary, based on both thermohaline properties. Application to the Ría de Arousa (NW Spain). Estuar Coast Shelf Sci 44:249–262

Rosón G, Pérez FF, Álvarez-Salgado XA, Pérez FF, Figueiras FG (1995) Variation of both thermohaline and chemical properties in an estuarine upwelling ecosystem: Ría de Arousa. I. Temporal evolution. Estuar Coast Shelf Sci 41: 195–213

Rosón, G, Pérez FF, Álvarez-Salgado XA, Ríos AF (1991) Flujos de los aportes de agua continental a la Ría de Arosa. Sci Mar 55(4):583–589

Simpson JJ, Zirino A (1980) Biological control of pH in the Peruvian coastal upwelling area. Deep-Sea Res 27: 733–744

Smith RL (1983) Circulation patterns in upwelling regimes. In: Suess E, Thiede J (eds) Coastal upwelling. Plenum Press, New York, p 13–35

Spencer CP (1975) The micronutrient elements. In: Riley JP, Skirrow G (eds) Chemical oceanography. Academic Press, London, p 245–300

Takahashi T, Goddard J, Sutherland S, Chipman DW, Breeze CC (1986) Seasonal and geographic variability of carbon dioxide sink/source in oceanic areas: observations in the North and Equatorial Pacific Ocean, 1984–1986 and global summary. In: DOE Technical Report MRETTA 19X-89675C. Lamont-Doherty Geological Observatory, Palisades, New York, p 1–52

Tenore KR and 18 co-authors (1982) Coastal upwelling in the Rías Baixas, NW Spain: contrasting the benthic regimes of the Rías de Arousa and Muros. J Mar Res 40:701–772

Walsh JJ (1991) Importance of continental margins in the marine biogeochemical cycling of carbon and nitrogen. Nature 350:53–55

Watson AJ, Robertson JE, Ling RD (1993) Air-sea exchange of CO_2 and its relation to primary production. In: Wollast R, Mackenzie FT, Chou L (eds) Interactions of C, N, P and S biogeochemical cycles and global change. NATO ASI Series 14, Springer-Verlag, Berlin, p 249–257

Weiss RF (1974) Carbon dioxide in water and seawater: the solubility of a non ideal gas. Mar Chem 2:203–215

Wollast R (1991) The coastal organic carbon cycle: fluxes, sources and sinks. In: Mantoura RFC, Martin JM, Wollast R (eds) Ocean margin processes in global change. J Wiley & Sons, Chichester, p 365–381

Wollast R (1993) Interactions of carbon and nitrogen cycles in the coastal zone. In: Wollast R, Mackenzie FT, Chou L (eds) Interactions of C, N, P and S biogeochemical cycles and global change, NATO ASI Series 14, Springer-Verlag, Berlin, p 195–210

Woolf DK, Thorpe SA (1991) Bubbles and the air-sea exchange of gases in near-saturation conditions. J Mar Res 49:435–466

Wooster WS, Bakun A, McClain DR (1976) The seasonal upwelling cycle along the eastern boundary of the North Atlantic. J Mar Res 34:131–141

Wroblewski JS, Hoffmann EE (1989) U.S. interdisciplinary modelling studies of coastal-offshore exchange processes: past and future. Prog Oceanogr 23: 65–99

Zimmerman RC, Kremer JN, Dugdale RC (1987) Acceleration of nutrient uptake by phytoplankton in a coastal upwelling ecosystem: a modelling analysis. Limnol Oceanogr 32: 359–367

Editorial responsibility: Otto Kinne (Editor), Oldendorf/Luhe, Germany

Submitted: November 11, 1997; Accepted: July 31, 1998
Proofs received from author(s): December 21, 1998